RESEARCH ARTICLE

Fabrication of high thermal conductivity copper/diamond composites by electrodeposition under potentiostatic conditions

Susumu Arai[1] · Miyoka Ueda[1]

Abstract

High thermal conductivity Cu/diamond composites were fabricated using an electrodeposition technique. The electrodes were oriented horizontally, and the cathode was located at the bottom of the plating bath. Diamond particles (10–230 µm) were first precipitated on the cathode substrate, and then copper was electrodeposited on the substrate to fill the gap between the precipitated diamond particles, which resulted in the formation of a Cu/diamond composite. The deposition behavior of the copper was electrochemically investigated, and the current densities of copper deposition under galvanostatic conditions were estimated. The current densities for the substrate with diamond particle layers were 4–10 times higher than the current density for the substrate without diamond particle layers, which led to undesired hydrogen evolution. Cu/diamond composites were formed under potentiostatic conditions without hydrogen evolution, and the resultant composites had compact morphologies. A specimen containing 49 vol% diamond particles with a mean diameter of 230 µm had the highest thermal conductivity of 600 W m^{-1} K^{-1}, which is 1.5 times that of pure copper (ca. 400 W m^{-1} K^{-1}).

Graphic Abstract

High thermal conductivity Cu/diamond composites were fabricated by electrodeposition under a potentiostatic condition without the evolution of hydrogen gas.
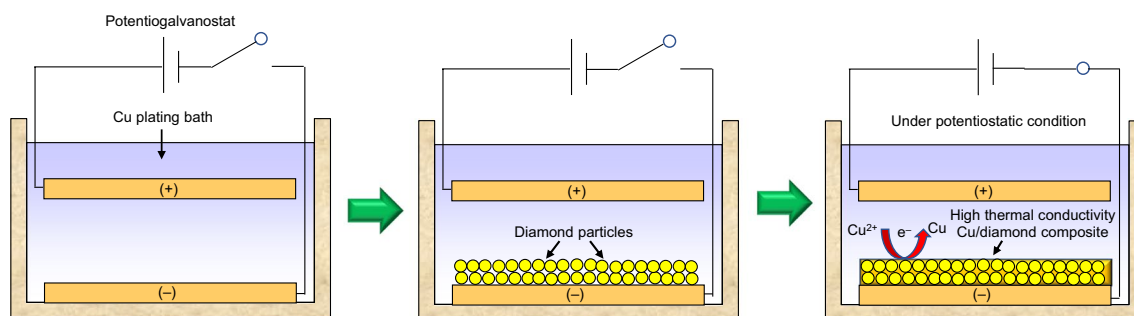
Keywords Copper · Diamond · Composite · Thermal conductivity · Electrodeposition · Galvanostatic condition · Potentiostatic condition

✉ Susumu Arai
araisun@shinshu-u.ac.jp

1   Department of Materials Chemistry, Faculty of Engineering, Shinshu University, 4-17-1 Wakasato, Nagano-shi, Nagano 380-8553, Japan

1 Introduction

Diamond has very high thermal conductivity, second only to that of carbon nanotubes (CNTs) [1–6]. However, the thermal conductivity of CNTs is also highly anisotropic due to their unique structure [2]. In contrast, diamond particles typically have a granular morphology and exhibit more isotropic thermal conductivity. For this reason,

diamond particles are expected to be applicable as raw materials for the preparation of high thermal conductivity composite materials, and there has been much research regarding the fabrication of composites comprising diamond together with Al [7, 8], Ag [9], or Cu [10–17]. Sintering and infiltration have traditionally been used to form such materials, although both methods require the application of extremely high temperatures and pressures. Moreover, metals such as Ag and Cu in the molten state are not able to readily wet diamond. Consequently, gaps or cracks tend to form between the metal matrix and the diamond particles in the composite, such that the resultant thermal conductivity is lower than that of the original metal. Both the wettability and thermal conductivity can be improved by pre-coating the diamond particles with the metal [2, 18–22], although the formation process is complicated and still requires the application of extremely high temperatures and pressures.

Electrodeposition could potentially be used to form metal layers on solid materials at ambient temperature and pressure, and thus could be advantageous. An investigation on the thermal conductivity of Cu/diamond composite materials fabricated using this technique has been reported recently [23]. Our group has also reported the excellent thermal conductivity of Cu/diamond composites formed by electrodeposition [24]. In both studies, the electrodes were arranged horizontally with the cathode at the bottom of a plating bath. Diamond particles were first precipitated on the cathode, after which copper was electrodeposited on the cathode to fill the gaps between the precipitated diamond particles, as well as between the substrate and the diamond particles. Furthermore, in both reports, electrodeposition was performed under galvanostatic conditions; i.e., the current density changes during electrodeposition. In some cases, the current density becomes sufficiently high to allow hydrogen gas evolution, which disturbs the arrangement of the precipitated diamond particles. Therefore, a copper electrodeposition technique that avoids hydrogen gas evolution is required.

In this study, the copper electrodeposition behavior, i.e., the current density, on a cathode with precipitated diamond particles was studied electrochemically under galvanostatic conditions. High thermal conductivity Cu/diamond composites were then fabricated without the evolution of hydrogen gas under potentiostatic conditions.

2 Experimental

Figure 1 shows the experimental procedure for the fabrication of Cu/diamond composites using electrodeposition. The electrodes were arranged horizontally with the cathode at the bottom. Diamond particles were first precipitated on the cathode, and then electrodeposition was performed to fill the gaps between the precipitated diamond particles, and between the substrate and precipitated diamond particles. Commercially available single-crystal diamond particles with various mean sizes (MMP series with 10, 25, and 45 μm sizes and SXD series with and 230 μm sizes, Changsha Xinye Co., Ltd.) were used. Scanning electron microscopy (SEM) images of the diamond particles are shown in Fig. 2. An aqueous solution containing 0.85 M $CuSO_4 \cdot 5H_2O$ and 0.55 M H_2SO_4 was employed as the copper plating bath. A pure copper plate and a copper plate containing phosphorus with an exposed surface area of 18 cm^2 (3×6 cm), were used as the cathode and anode, respectively. The electrolytic cell was constructed of an acrylic resin and its internal dimensions were $3.5 \times 7 \times 6$ cm. The masses of the 10, 25, 45, and 230 μm diamond particles added to the bath were approximately 0.11, 0.28, 0.50, and 2.53 g, respectively, which correspond to two layers of particles (a bilayer) on the cathode. In the case of a monolayer, half the amount of diamond particles was added to the bath. These masses were estimated using the diamond density and the diamond particle sizes. Before electrodeposition, the diamond particles were dispersed homogeneously using a stirring bar and left undisturbed to
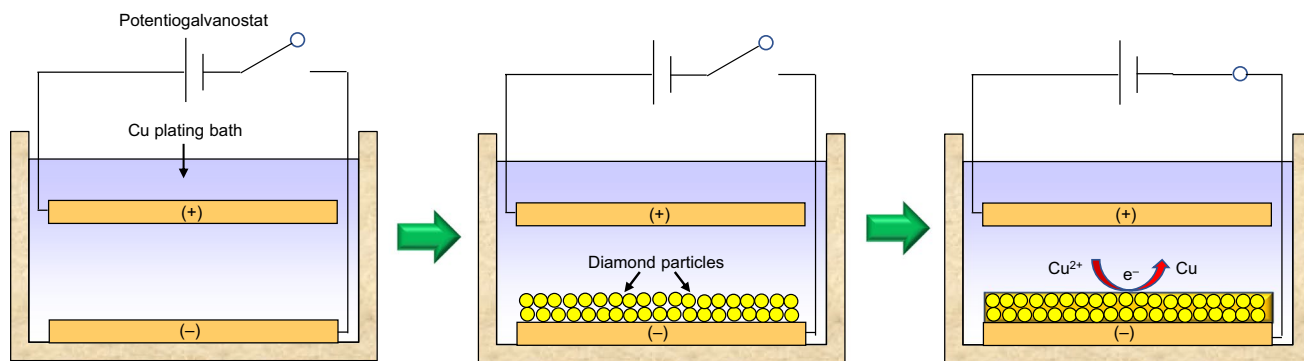
Fig. 1 Schematic illustration of the process for fabrication of Cu/diamond composites using electrodeposition

Fig. 2 SEM images of diamond particles used: **a** 10 μm, **b** 25 μm, **c** 45 μm, and **d** 230 μm
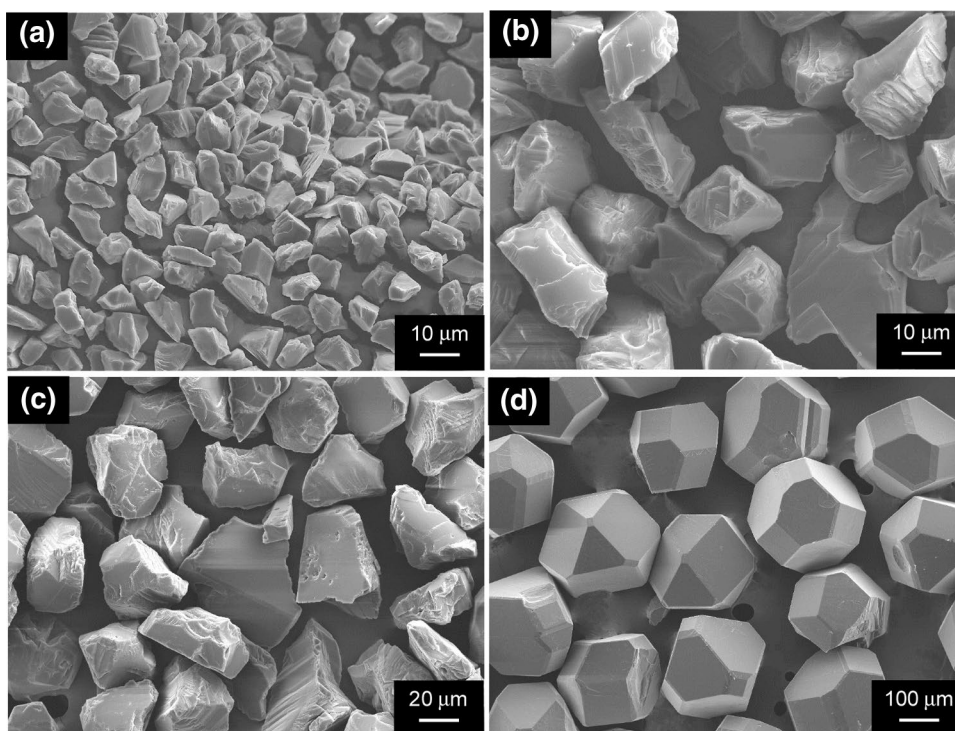
allow the diamond particles to precipitate, i.e., to arrange diamond particle layer(s) on the cathode. In the case of a bilayer, the quantities of electrical charge passed through the cell were 54, 135, 243, and 1240 C cm^{-2}.

The electrodeposition process fills the gaps between the precipitated diamond particles, and between the substrate and precipitated diamond particles; therefore, the surface area of deposited copper, and thus the current density, should change during electrodeposition under galvanostatic conditions. Electrochemical measurements were conducted at 25 °C using an electrochemical measurement system (HZ-5000 Hokuto Denko Co. Ltd.) to estimate the current densities during electrodeposition under galvanostatic conditions. Measurements of the rest potential and current-potential curve, and chronoamperometry were conducted using a pure copper plate, a copper plate containing phosphorus, and a saturated calomel electrode (SCE) as the working, counter, and reference electrodes, respectively. Current-potential curves were obtained at 50 mV min^{-1}. Chronoamperometry was performed in the overpotential range of 50–260 mV for 600 s to obtain steady-state current densities that corresponded to the overpotentials. Chronopotentiometry was conducted for the cathode with a diamond particle layer under galvanostatic conditions (90 mA: 5 mA cm^{-2} for the cathode substrate without diamond particle layers). Electrodeposition of copper was also conducted under potentiostatic conditions at -0.20 V vs. SCE (0.0412 V vs. standard hydrogen electrode (SHE), at which hydrogen evolution cannot occur) on the cathode with a diamond particle layer.

The diamond content (vol%) in each composite formed was determined by directly weighing the specimens after removal of the copper matrix with HNO_3. The surface and cross-sectional morphologies of the composites were examined using field-emission SEM (FE-SEM, SU-8000, Hitachi High Technologies Co.), with samples prepared using a cross-section polisher (SM-09010, JEOL Ltd.). The thermal diffusivity (α) of each specimen was measured with a xenon laser flash thermal properties analyzer (LFA 447-2 Nanoflash, Netzsch Co., Ltd.). The α values of the Cu/diamond composite samples fabricated with 10, 25, and 45 μm diamond particles were measured in the thin film, in plain mode, while the specimen formed with 230 μm particles was assessed in the bulk, in normal mode. The density (ρ_{comp}) and specific heat capacity (C_{comp}) of each composite were calculated using the following equations: [10–13]

$$\rho_{comp} = \rho_{dia} \cdot V_{dia} + \rho_{Cu} \cdot V_{Cu} \tag{1}$$

and

$$C_{comp} = \frac{C_{dia} \cdot V_{dia} \cdot \rho_{dia} + C_{Cu} \cdot V_{Cu} \cdot \rho_{Cu}}{\rho_{comp}}, \tag{2}$$

where ρ_{dia} and ρ_{Cu} are the densities of diamond (3.52 g dm^{-3}) and Cu (8.94 g dm^{-3}), V_{dia} and V_{Cu} are the experimentally determined volume percentages of diamond and copper, and C_{dia} and C_{Cu} are the specific heat capacities of diamond (0.512 J g^{-1} K^{-1}) and copper (0.385 J g^{-1} K^{-1}),

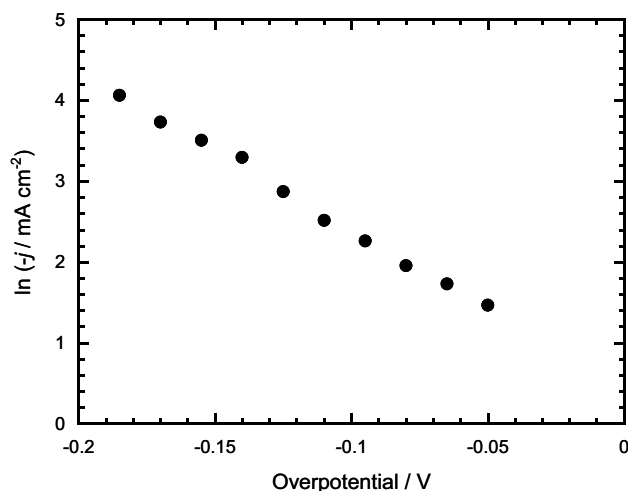respectively. The thermal conductivity (λ_{comp}) of each sample was calculated as according to

$$\lambda_{comp} = \alpha \cdot \rho_{comp} \cdot C_{comp}. \tag{3}$$

3 Results and discussion

Figure 3 shows an overpotential-current density curve for the electrodeposition of copper on a copper substrate without a diamond particle layer measured in the sulfate plating bath. The limiting current density was ca. -120 mA cm^{-2}, and significant hydrogen evolution began at overpotentials greater than ca. -0.6 V. Hydrogen evolution during electrodeposition on the cathode with diamond particle layers would disturb the layer arrangement; therefore, electrodeposition should be conducted at a current density of less than -120 mA cm^{-2} or at an overpotential lower than -0.6 V. During the electrodeposition of copper on the cathode with diamond particle layers under galvanostatic conditions, the cathode surface area changes, which results in a change in the current density. Diamond particles with undefined shape were used in this study (Fig. 2); therefore, the surface area of the electrodeposited copper was unclear, and consequently, the current density was ambiguous. Electrochemical techniques were employed to estimate the current density during copper electrodeposition. Figure 4 shows a Tafel plot for the electrodeposition of copper on a copper cathode without diamond particle layers. The plot was linear in the overpotential range of -0.05 to ca. -0.20 V, whereas good linearity was not obtained at overpotentials higher than ca. -0.20
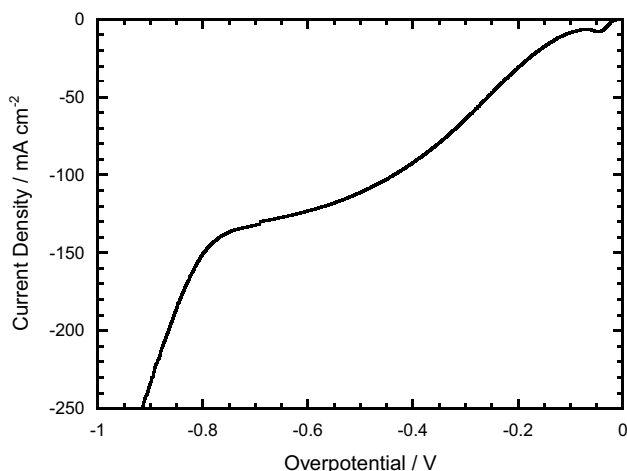
Fig. 4 Tafel plot for the electrodeposition of copper on a copper cathode without diamond particle layers

V. Therefore, a charge transfer process is considered to be the main rate-limiting step in the potential range up to ca. -0.20 V, while both mass transfer and charge transfer processes significantly affect the electrodeposition rate of copper at potentials greater than ca. -0.20 V. It is generally accepted that copper electrodeposition from acidic sulfate solutions proceeds as follows:

$$Cu^{2+} + e^- \rightleftharpoons Cu^+ \quad E° = 0.16 \text{ V vs. SHE} \tag{4}$$

$$Cu^+ + e^- \rightleftharpoons Cu \quad E° = 0.52 \text{ V vs. SHE} \tag{5}$$

where the first process is the rate-determining step [25]. In the case of large cathode overpotentials over -0.12 V (-0.05 V is acceptable), the following relationship exists between the current density (j) and overpotential (η):

$$\ln(-j) = \frac{-\alpha nF}{RT}\eta + \ln j_0, \tag{6}$$

where α is the transfer coefficient, n is the number of electrons involved in the rate-determining step (in this case $n = 1$), F is the Faraday constant, R is the gas constant, T is the absolute temperature, and j_0 is the exchange current density. Least-squares fitting of the Tafel plot in the potential range of -0.05 to -0.125 V to Eq. 6 yielded values of $\alpha = 0.47$ and $j_0 = 1.7$ mA cm^{-2}, which were almost the same as those previously reported in the literature [26]. The value of j_0 obtained in this study is somewhat larger than the previously reported values (1.1–1.4 mA cm^{-2}), which is most likely due to the difference in the concentrations of Cu^{2+} ions in this study (0.85 M) and those in the previous study (0.25 M). The Tafel slope was 124 mV/decade, which is also similar to the literature values [27–29]. Substituting the obtained kinetic parameter values of α and j_0 into the
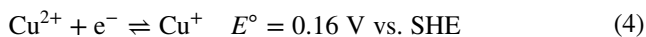

Fig. 3 Overpotential-current density curve for the electrodeposition of copper on a copper substrate without a diamond particle layer measured in the acidic copper plating bath

Butler–Volmer equation, the relationship between j (mA cm^{-2}) and η (V) was obtained as follows:

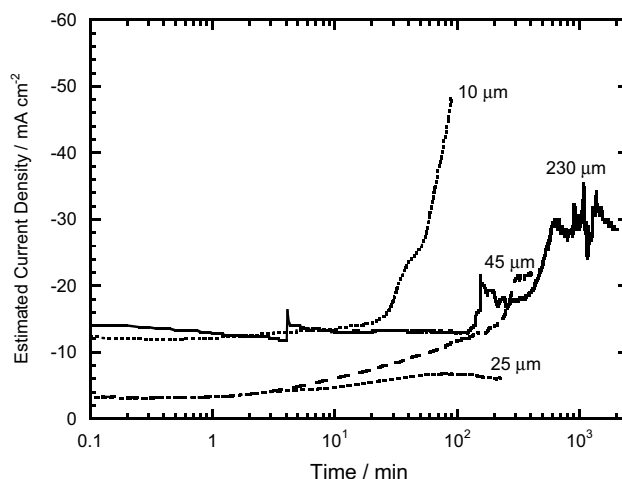$$j = 1.7\left(e^{20.6\eta} - e^{-18.2\eta}\right). \tag{7}$$

Figure 5 shows the overpotential transitions during copper electrodeposition on the copper substrate with diamond particle layer(s) at a current of 90 mA (5 mA cm^{-2} for the substrate without diamond particle layer). The overpotential during copper electrodeposition on the copper substrate without a diamond particle layer was ca. -0.05 V. In the case of the monolayer (Fig. 5a), the overpotentials were greater than -0.05 V. Accordingly, the overpotentials for all substrates with diamond particle monolayers were increased to some extent compared to that without a diamond particle layer. However, the overpotentials were lower than -0.20 V, and the fluctuations were relatively small for all diamond particle sizes. In contrast, for the bilayer (Fig. 5b), the
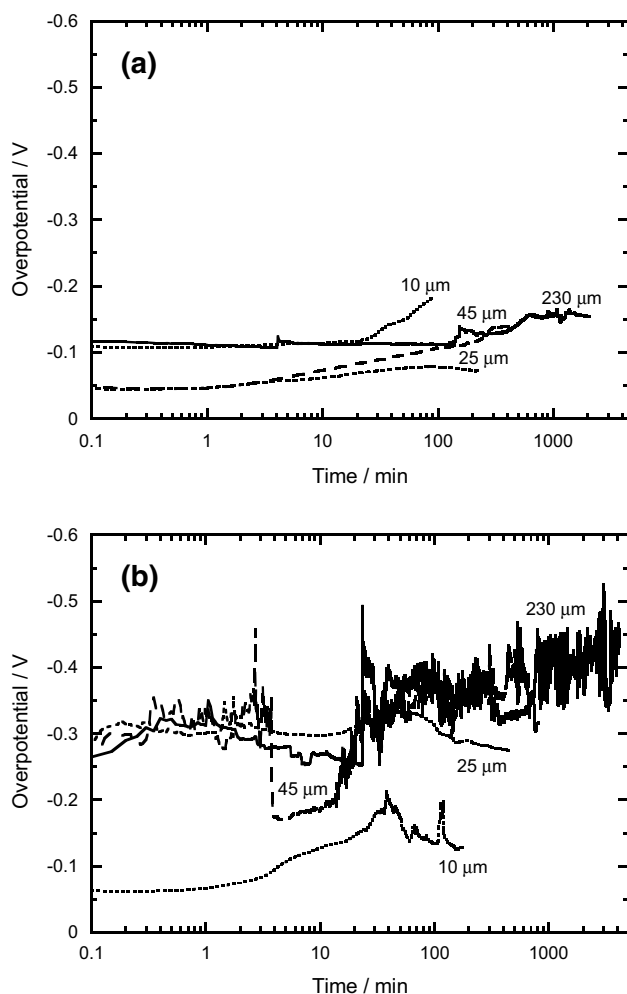
overpotentials and fluctuations were considerably larger than those for the monolayer. The overpotential for the substrate with 230 μm size diamond particle layers was occasionally greater than -0.50 V, at which there is a risk of considerable hydrogen evolution. Therefore, in the case of the monolayer where the overpotentials for all diamond particles sizes were lower than -0.20 V, the electrodeposition of copper should proceed mainly as a charge transfer process. Consequently, the conversion of the overpotentials to current densities is possible using Eq. 7. In contrast, the overpotentials for bilayers were considerably large (greater than -0.20 V), so that the electrodeposition of copper proceeds not only in charge-transfer mode but also in mass-transfer mode; therefore, Eq. 7 cannot be used to convert the overpotentials to current densities.

Figure 6 shows the estimated current density transition during the electrodeposition of copper on a substrate with a diamond monolayer using the data from Fig. 5a and Eq. 7. The estimated current density during the electrodeposition of copper on the substrate without diamond layers was ca. 4 mA cm^{-2}. For the 10 μm diamond particles, the current density reached 50 mA cm^{-2}, which is 10 times higher than that for the copper substrate without diamond particles (5 mA cm^{-2}). Therefore, the electrodeposition of copper under galvanostatic conditions on the substrate with a diamond particle layer(s) was difficult to control, so that copper electrodeposition under potentiostatic conditions was examined. Figure 7 shows current-potential curve for copper electrodeposition, where the x-axis has been converted to the potential versus SHE from SCE (Fig. 3). To completely avoid hydrogen evolution during copper deposition, the potential was set to 0.0412 V vs. SHE (-0.200 V vs. SCE). The corresponding current density was ca. -55 mA cm^{-2}.
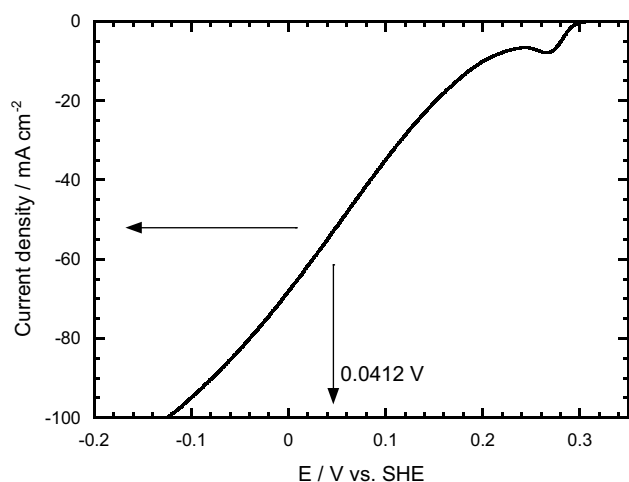

Fig. 5 Overpotential as a function of time during copper deposition on the substrate with diamond particle layer(s) at 5 mA cm^{-2} for various diamond particle sizes: **a** monolayer and **b** bilayer

Fig. 6 Estimated current densities as a function of time during copper deposition on a substrate with a diamond monolayer at 5 mA cm^{-2}

Fig. 7 Current-potential curve for copper deposition. The x-axis has been converted from potential vs. SCE to potential vs. SHE

Figure 8 shows surface SEM images of Cu/diamond composites fabricated under potentiostatic conditions. The diamond particles are a bilayer. The deposited copper fills the gaps between the diamond particles, which resulted in Cu/diamond composites for all diamond sizes. Figure 9 shows a cross-sectional SEM image of the Cu/diamond composite, where the dark regions are the 45 µm diamond particles. The diamond particles were embedded in the deposited copper, and there were no gaps between the copper matrix and diamond particles. Therefore, the Cu/diamond composites

fabricated by electrodeposition under potentiostatic conditions are considered to have a dense morphology.

Table 1 shows the composition of the Cu/diamond composites formed and their thermal conductivities. Theoretical values were calculated using the Hasselman–Johnson equation: [30]

$$\lambda_{sim} = \lambda_{Cu}\left\{\frac{2\left(\frac{\lambda_{dia}}{k_{Cu}} - \frac{\lambda_{dia}}{ah_c} - 1\right)V_{dia} + \frac{\lambda_{dia}}{\lambda_{Cu}} + \frac{2\lambda_{dia}}{ah_c} + 2}{\left(1 - \frac{\lambda_{dia}}{\lambda_{Cu}} + \frac{\lambda_{dia}}{ah_c}\right)V_d + \frac{\lambda_{dia}}{\lambda_{Cu}} + \frac{2\lambda_{dia}}{ah_c} + 2}\right\}, \quad (8)$$

where λ_{sim} is the simulated thermal conductivity of the Cu/diamond composite, λ_{dia} is the thermal conductivity of diamond, λ_{Cu} is the thermal conductivity of Cu, a is the mean radius of the diamond particles, V_{dia} is the volume percentage of the diamond particles, and h_c is the boundary conductance between the Cu matrix and diamond particles. In this simulation, λ_{dia}, λ_{Cu}, and h_c were assumed to be 1300 W m^{-1} K^{-1} [10, 18], 400 W m^{-1} K^{-1}, and 8.86×10^8 W m^{-2} K^{-1} [31]. The thermal conductivities of Cu/diamond composites with diamond particle sizes larger than 25 µm were higher than that of pure copper (400 W m^{-1} K^{-1}). In particular, the thermal conductivity of the Cu/diamond composite with 230 µm diamond particles (49 vol%) reached 600 W m^{-1} K^{-1}, which is 1.5 times that of pure copper. Experimentally measured thermal conductivities roughly corresponded to the simulated thermal conductivities, which indicates that the Cu/diamond composites fabricated in this study have

Fig. 8 Surface SEM images of Cu/diamond composites with various diamond particle sizes fabricated by electrodeposition under potentiostatic conditions (– 0.200 V vs. SCE, or − 0.0412 V vs. SHE): **a** 10 µm, **b** 25 µm, **c** 45 µm, and **d** 230 µm
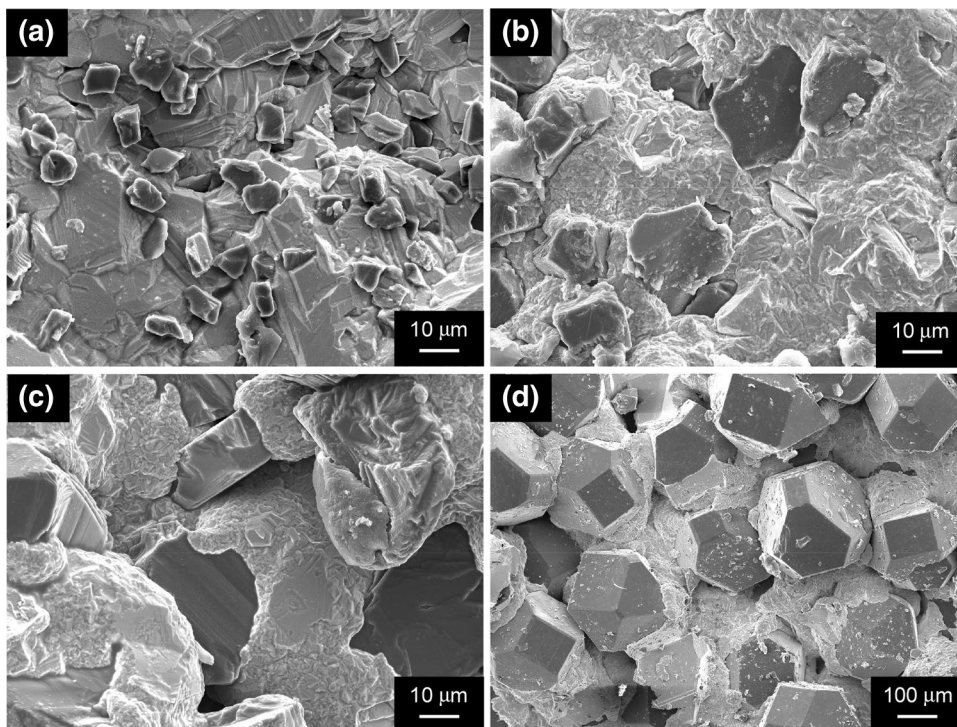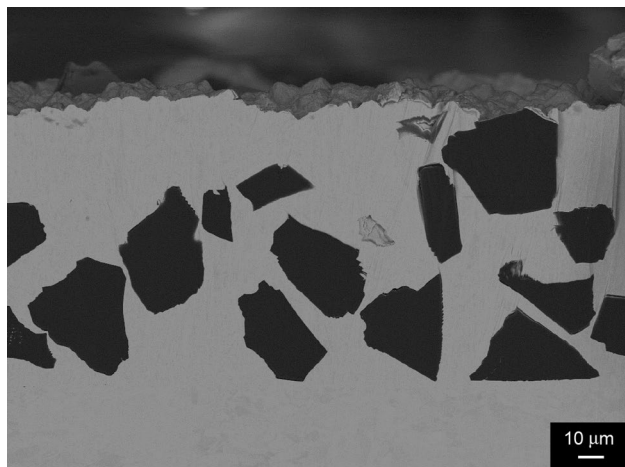
Fig. 9 Cross-sectional SEM image of a Cu/diamond composite with 45 μm diamond particles prepared under potentiostatic conditions (–0.200 V vs. SCE, or −0.0412 V vs. SHE)

Table 1 Compositions and thermal conductivities of Cu/diamond composites fabricated under potentiostatic conditions (0.0412 V vs. SHE)

Diamond particle size (μm)	Volume fraction of diamond (%)	Thermal conductivity: measured (W m^{-1} K^{-1})	Thermal conductivity: theoretical (W m^{-1} K^{-1})
10	14	385	390
25	31	424	455
45	32	469	502
230	49	600	679

close to ideal textures for use as high thermal conductivity materials. Electrodeposition under potentiostatic conditions can thus be considered as an excellent method for the fabrication of high thermal conductivity Cu/diamond composites, and this strategy could be extended to other metal/diamond composites.

4 Summary

Cu/diamond composites with high thermal conductivities were fabricated using an electrodeposition technique. The electrodes were arranged horizontally and the cathode was positioned at the bottom of the plating bath. Diamond particles (10–230 μm) were first precipitated on the cathode substrate, and copper was then electrodeposited to fill the gaps between the precipitated diamond particles, and between the substrate and the diamond particles, which resulted in Cu/diamond composites. The current densities during electrodeposition on the substrate with a diamond particle layer(s) were estimated electrochemically under galvanostatic

conditions. The measured current densities for a substrate with a diamond monolayer were several times higher than that for a substrate without a diamond particle layer, which implies the risk of hydrogen evolution. The Cu/diamond composites formed under potentiostatic conditions where hydrogen evolution cannot occur (+0.0412 V vs. SHE) had compact morphologies with no gaps between the copper matrix and the diamond particles. The highest thermal conductivity measured was that for the Cu/diamond composite containing 49 vol% of 230 μm diamond particles, which reached 600 W m^{-1} K^{-1} or 1.5 times that of pure copper.

References

1. Ho CY, Powell RW, Liley PE (1972) Thermal conductivity of the elements. J Phys Chem Data 1:318
2. Abyzov AM, Kindalov SV, Shakhov FM (2011) High thermal conductivity composites consisting of diamond filler with tungsten coating and copper (silver) matrix. J Mater Sci 46:1424–1438
3. Berber S, Kwon YK, Tomanek D (2000) Unusually high thermal conductivity of carbon nanotubes. Phys Rev Lett 84:4613–4616
4. Cao A, Qu J (2012) Size dependent thermal conductivity of single-walled carbon nanotubes. J Appl Phys 112:013503
5. Yu CH, Shi L, Yao Z, Li DY, Majumdar A (2005) Thermal conductance and thermopower of an individual single-wall carbon nanotube. Nano Lett 5:1842–1846
6. Kim P, Shi L, Majumdar A, McEuen PL (2001) Thermal transport measurements of individual multiwalled nanotubes. Phys Rev Lett 87:215502
7. Feng H, Yu JK, Tan W (2010) Microstructure and thermal properties of diamond/aluminum composites with TiC coating on diamond particles. Mater Chem Phys 124:851–855
8. Mizuuchi K, Inoue K, Agari Y, Morisada Y, Sugioka M, Tanaka M, Takeuchi T, Kawahara M, Makino Y (2011) Thermal conductivity of diamond particle dispersed aluminum matrix composites fabricated in solid-liquid co-existent state by SPS. Compos B 42:1029–1034
9. Lee MT, Fu MH, Wu JL, Chung CY, Lin SJ (2011) Thermal properties of diamond/Ag composites fabricated by electroless silver plating. Diam Relat Mater 20:130–133
10. Yoshida K, Morigami H (2004) Thermal properties of diamond/copper composite material. Microelectron Reliab 44:303–308
11. Weber L, Tavangar R (2007) On the influence of active element content on the thermal conductivity and thermal expansion of Cu-X (X = Cr, B) diamond composites. Scr Mater 57:988–991

12. Ekimov EA, Suetin NV, Popovich AF, Ralchenko VG (2008) Thermal conductivity of diamond composites sintered under high pressures. Diam Relat Mater 17:838–843

13. Dong YH, He XB, Din RU, Xu L, Qu XH (2011) Fabrication and thermal conductivity of near-net-shaped diamond/copper composites by pressureless infiltration. J Mater Sci 46:3862–3867

14. Bai H, Ma N, Lang J, Zhu C (2013) Effect of a new pretreatment on the microstructure and thermal conductivity of Cu/diamond composites. J Alloys Compd 580:382–385

15. Raza K, Khalid FA (2014) Optimization of sintering parameters for diamond-copper composites in conventional sintering and their thermal conductivity. J Alloys Compd 615:111–118

16. Wang HY, Tian J (2014) Thermal conductivity enhancement in Cu/diamond composites with surface-roughed diamonds. Appl Phys A 116:265–271

17. Mankowski P, Dominiak A, Domanski R, Kruszewski M, Ciupinski L (2014) Thermal conductivity enhancement of copper-diamond composites by sintering with chromium additive. J Therm Anal Calorim 116:881–885

18. Chu K, Liu Z, Jia C, Chen H, Liang X, Gao W, Tian W, Guo H (2010) Thermal conductivity of SPS consolidated Cu/diamond composites with Cr-coated diamond particles. J Alloys Compd 490:453–458

19. Ren S, Shen X, Guo C, Liu N, Zang J, He X, Qu X (2011) Effect of coating on the microstructure and thermal conductivities of diamond-Cu composites prepared by powder metallurgy. Compos Sci Technol 71:1550–1555

20. Abyzov AM, Kidalov SV, Shakhov FM (2012) High thermal conductivity composite of diamond particles with tungsten coating in a copper matrix for heat sink application. Appl Therm Eng 48:72–80

21. Shen XY, He XB, Ren SB, Zhang HM, Qu XH (2012) Effect of molybdenum as interfacial element on the thermal conductivity of diamond/Cu composites. J Alloys Compd 529:134–139

22. Kang Q, He X, Ren S, Zhang L, Wu M, Liu T, Liu Q, Gu C, Qu X (2013) Preparation of high thermal conductivity copper-diamond composites using molybdenum carbide-coated diamond particles. J Mater Sci 48:6133–6140

23. Cho HJ, Yan D, Tam J, Erb U (2019) Effects of diamond particle size on the formation of copper matrix and the thermal transport properties in electrodeposited copper-diamond composite materials. J Alloys Compd 797:122–130

24. Arai S, Ueda M (2019) Fabrication of high thermal conductivity Cu/diamond composites at ambient temperature and pressure. AIP Adv 9:085309

25. Mattson E, Bockris OM (1959) Galvanostatic studies of the kinetics of deposition and dissolution in the copper + copper sulphate system. Trans Faraday Soc 55:1586–1601

26. Moffat TP, Wheeler D, Josell D (2004) Electrodeposition of copper in the SPS-PEG-Cl additive system I. Kinetic measurements: influence of SPS. J Electrochem Soc 151:C262–C271

27. Varvara S, Muresan L, Nicoara A, Maurin G, Popescu IC (2001) Kinetic and morphological investigation of copper electrodeposition from sulfate electrolytes in the presence of an additive based on ethoxyacetic alcohol and triethyl-benzyl-ammonium chloride. Mater Chem Phys 72:332–336

28. Doblhofer K, Wasle S, Soares DM, Weil KG, Weinberg G, Ertl G (2003) The influence of halide ions on the kinetics of electrochemical copper (II) reduction. Z Phys Chem 217:479–491

29. Shao W, Pattanaik G, Zangari G (2007) Influence of chloride anions on the mechanism of copper electrodeposition from acidic sulfate electrolytes. J Electrochem Soc 154:D201–D207

30. Hasselman DPH, Johnson LF (1987) Effective thermal conductivity of composites with interfacial thermal barrier resistance. J Compos Mater 21:508–515

31. Wang H, Xu Y, Shimono M, Tanaka Y, Yamazaki M (2007) Computation of interfacial thermal resistance by phonon diffuse mismatch model. Mater Trans 48:2349–2352